

Facile Synthesis of Highly Fluorescent Boranil Complexes

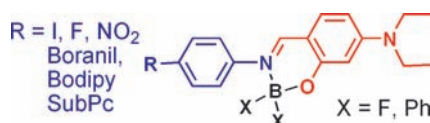
Denis Frath,[†] Sébastien Azizi,[†] Gilles Ulrich,^{*,†} Pascal Retailleau,[‡]
and Raymond Ziessel^{*,†}

Laboratoire de Chimie Organique et Spectroscopies Avancées (LCOSA),
UMR7515 au CNRS, Ecole de Chimie, Polymères, Matériaux de Strasbourg (ECPM),
25 rue Becquerel, 67087 Strasbourg, Cedex 02, France, and Laboratoire de Crystallochimie,
ICSN - CNRS, Bât 27 - 1 avenue de la Terrasse, 91198 Gif-sur-Yvette, Cedex, France

ziessel@unistra.fr

Received May 2, 2011

ABSTRACT



Complexation of a large variety of *Anils* (aniline-imines) with boron(III) precursors provides stable *Boranils*, some of which have been structurally characterized. Analysis of their optical properties reveals that the fluorescence stems from an intraligand charge transfer (ILCT) state with the best quantum yields reaching 90%. Chemistry on the *Boranils* allows grafting of photoactive modules acting as energy antennae for borondipyrromethene (Bodipy) and subphthalocyanine (SubPc) fluorophores.

To date, considerable effort has been devoted to the development of innovative fluorescent dyes for applications as labels in biomedical analysis,¹ molecular sensors,² and light emitting devices.³ Efficient photoluminescence and ambipolar charge transport properties have been reported for some of these dyes.⁴ Of the many conventional fluorophores, those of the Bodipy family are most intriguing due to their outstanding optical properties, extraordinary chemical versatility, and variety of applications

spanning from biolabeling⁵ to solar cells⁶ and nanoparticle engineering.⁷ Yet, despite these attractive features, the synthesis of such dyes remains tedious, involving linear stepwise syntheses with relatively low global yields. Thus, it is significant to note that other N[^]N[^] bidentate ligands (e.g., deprotonated benzimidazoles, indoles, azaindoles, and pyrazoylanilines) form stable boron complexes with interesting luminescence properties.⁸

The search for alternative fluorescent dyes prompted us to envisage changes in, first, the nature of the chelate unit and, second, the nature of the B(III) fragment [BF₂, B(Ar)₂, B(ArF₅)₂, B(OAr)₂]. Coordinately saturated (and essentially tetrahedral) B complexes have been studied using N[^]N[^]O[^]O[^]-tetradentate ligands,⁹ O[^]N[^]O[^] tridentate ligands,¹⁰ or N[^]O[^]-bidentate ligands (Figure 1). This group can be divided into those forming five-membered rings with quinolines¹¹ or six-membered rings with salicylaldehydes,¹² oxazolylphenolates,¹³ acylpyrrole,¹⁴ or pyridinephenolates.¹⁵

[†]LCOSA, CNRS, ECPM.

[‡]Laboratoire de Crystallochimie, ICSN - CNRS.

(1) (a) Yang, W.; He, H.; Drueckhammer, D. G. *Angew. Chem., Int. Ed.* **2001**, *40*, 1714. (b) Killoran, J.; Allen, L.; Gallagher, J. F.; Gallagher, W. M.; O'Shea, D. F. *Chem. Commun.* **2002**, 1862.

(2) (a) Beer, G.; Niederalt, C.; Grimme, S.; Daub, J. *Angew. Chem. Int. Ed.* **2000**, *39*, 3252. (b) Yamaguchi, S.; Akiyama, S.; Tamao, K. *J. Am. Chem. Soc.* **2001**, *123*, 11372. (c) Shigehiro, Y.; Toshiaki, S.; Seiji, A.; Kohei, J. *J. Am. Chem. Soc.* **2002**, *124*, 8816.

(3) (a) Shirota, Y.; Kinoshita, M.; Noda, T.; Okumoto, K.; Ohara, T. *J. Am. Chem. Soc.* **2000**, *122*, 11021. (b) Wang, S. *Coord. Chem. Rev.* **2001**, *215*, 79. (c) Liu, Y.; Guo, J. H.; Zhang, H. D.; Wang, Y. *Angew. Chem., Int. Ed.* **2002**, *41*, 182.

(4) Noda, T.; Ogawa, H.; Shirota, Y. *Adv. Mater.* **1999**, *11*, 283.

(5) Wu, L.; Loudet, A.; Barhoumi, R.; Burghardt, R.; Burgess, K. *J. Am. Chem. Soc.* **2009**, *131*, 9156.

(6) (a) Erten-Ela, S.; Yilmaz, D.; Icli, B.; Dede, Y.; Icli, S.; Akkaya, U. E. *Org. Lett.* **2008**, *10*, 3299. (b) Kumaresan, D.; Thummel, R. P.; Bura, T.; Ulrich, G.; Ziessel, R. *Chem.—Eur. J.* **2009**, *15*, 6335. (c) Rousseau, T.; Cravino, A.; Ripaud, E.; Leriche, P.; Rihn, S.; De Nicola, A.; Ziessel, R.; Roncali, J. *Chem. Commun.* **2010**, *46*, 5082.

(7) Tokoro, Y.; Nagai, A.; Chujo, Y. *Tetrahedron Lett.* **2010**, *51*, 3451.

(8) (a) Liu, Q.; Mudadu, M. S.; Schmider, H.; Thummel, R.; Tao, Y.; Wang, S. *Organometallics* **2002**, *21*, 4743. (b) Liu, Q.-D.; Mudadu, M. S.; Thummel, R.; Tao, Y.; Wang, S. *Adv. Funct. Mater.* **2005**, *15*, 143.

(9) Kim, H.; Burghart, A.; Welch, M. B.; Reibenspies, J.; Burgess, K. *Chem. Commun.* **1999**, 1889.

(10) (a) Kaiser, P. F.; White, J. M.; Hutton, C. A. *J. Am. Chem. Soc.* **2008**, *130*, 16450. (b) Schlecht, S.; Frank, W.; Braun, M. *Eur. J. Org. Chem.* **2010**, 3721.

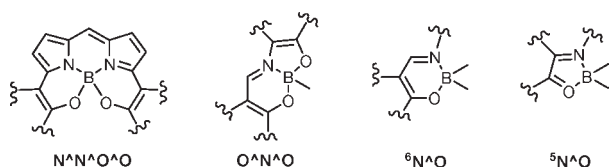


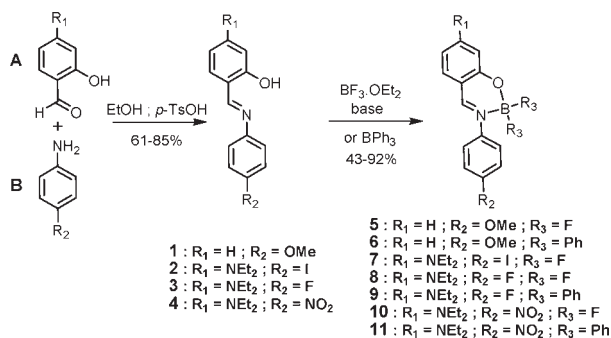
Figure 1. Various chelating modes of B(III) complexes.

More exotic N,O-chelates forming six-membered rings have been obtained from phenalene-1,3-dione and perylenediimides.¹⁶ Also, dinuclear B-complexes have been prepared with binaphthyl, salen, and para-phenyl frameworks.¹⁷ Yet, the luminescence quantum yields for such derivatives are typically low, and little information about their photostability is available.

Here we disclose the facile preparation in two steps of novel B(III) complexes of various substituted *Anils*, giving *Boranil* complexes bearing substituents engendering strong luminescence in both solution and the solid state. Such complexes offer interesting prospects because of their facile synthesis on a large scale from common precursors and their possible use as synthons for connection of an additional chromophoric subunit or other module of interest. Some of the complexes without donor/acceptor modules have previously been prepared.^{12a,18}

Preparation of the *Anil*¹⁹ derivatives **1–4** is straightforward starting from the aldehydes **A** and anilines **B** in refluxing ethanol with trace amounts of *p*-TsOH (Scheme 1). During the course of the reaction the desired imines precipitate pure out of the reaction mixture.

Scheme 1. Synthesis of the *Anils* and their *Boranil* Complexes



Subsequent B(III) complexation is feasible with BF₃·Et₂O under basic conditions (diisopropylethylamine) to quench the nascent HF or with BPh₃ in hot toluene. No base is required in this latter case, but the phenyl is used as the proton scavenger, producing benzene. The reactions were readily monitored by ¹H NMR spectroscopy, the loss of the signal near δ 13 ppm due to the intramolecularly H-bonded phenolic proton of

1–4 being distinctive. In the BF₂-containing products, coupling of the imine proton to B is observed, leading to the appearance of a broad quartet due to the ¹¹B coupling (³J_{H–B} = 3.7 Hz) (Figure S1). This coupling is absent in the BPh₂ analogues owing to the longer N–B distance as observed in the X-ray molecular structure (*vide infra*).

The X-ray molecular structures of **6** and **5** are shown in Figures 2 and 3, respectively, with selected geometric values. In both structures, the B has a slightly distorted tetrahedral geometry with angles ranging from 106.43(15)° and 115.31(16)° and from 104.6(11)° and 112.2(11)° in **6** and **5**, respectively. Surprisingly, the N₁^O₁ fragment appears *quasi*-planar in **6**, with an rms deviation of 0.0110 Å, while B1 lies only 0.0313(28) Å out of the least-squares mean plane defined by the nine atoms including N1 and O1. This is unlike any of the *II* structures of diphenylboron Schiff base derivatives found to date in the CSD,²⁰ in which all the chelate rings are markedly distorted from planarity. Such distortions are seen in the difluoroboron derivative **5**, where the B-atom is displaced 0.435(16) Å from the heterocycle mean plane. With the exception of the difluoroboron chelate of *N*-methyl salicylalimine,²¹ all six other structures of difluoroboron chelates found within the CSD also show strong distortions of the chelate rings from planarity.

The B1–O1 and B1–N1 distances are significantly longer in **6** than the corresponding distances in **5** (1.639(3) vs 1.503(3) Å and 1.552(15) vs 1.420(20) Å, respectively), presumably in reflection of the electronegativity of the fluorine substituents. As a consequence of the congested substitution at the B-center by two phenyl groups, the methoxyphenyl substituent at the N1 atom is more tilted in **6** than in **5**, as indicated by the respective dihedral angles between the least-squares mean plane defined by the heterobicycle and that of the phenyl ring, 63.46(9)° vs 48.70(60)°. The dihedral angles between the phenyl (C21/C26 and C15/C20) B-substituents and the heterobicycle in **6** are 58.57(9)° and 76.21(10)°, respectively. The crystal packing of both molecules is described in detail in the Supporting Information (Figure S2 and S3).

(12) (a) Umland, F.; Hohaus, E.; Brodte, K. *Chem. Ber.* **1973**, *106*, 2427. (b) Hohaus, E. *Monatsh. Chem.* **1980**, *111*, 863.

(13) Son, H.-J.; Han, W.-S.; Wee, K.-R.; Chun, J.-Y.; Choi, K.-B.; Han, S. J.; Kwon, S.-N.; Lee, C.; Kang, S. O. *Eur. J. Inorg. Chem.* **2009**, 1503.

(14) (a) Chen, J.; Burghart, A.; Wan, C.-W.; Thai, C.; Ortiz, J.; Reibenspies, J.; Burgess, K. *Tetrahedron Lett.* **2000**, *41*, 2303. (b) Muthukumar, K.; Ptaszek, M.; Noll, B.; Scheidt, W. R.; Lindsey, J. S. *J. Org. Chem.* **2004**, *69*, 5354. (c) Bhaumik, J.; Yao, Z.; Borbas, E.; Taniguchi, M.; Lindsey, J. S. *J. Org. Chem.* **2006**, *71*, 8807.

(15) Zhang, Z.; Bi, H.; Zhang, Y.; Yao, D.; Gao, H.; Fan, Y.; Zhang, H.; Wang, Y.; Wang, Y.; Chen, Z.; Ma, D. *Inorg. Chem.* **2009**, *48*, 7230.

(16) (a) Zhou, Y.; Chi, S.; Qian, X. *Org. Lett.* **2008**, *10*, 633. (b) Feng, J.; Lia, g. B.; Wang, D.; Xue, D.; Li, X. *Org. Lett.* **2008**, *10*, 4437.

(17) (a) Zhou, Y.; Kim, J. W.; Nandhakumar, R.; Kim, M. J.; Cho, E.; Kim, Y. S.; Jang, Y. H.; Lee, C.; Han, S.; Kim, K. M.; Kim, J.-J.; Yoon, Y. *Chem. Commun.* **2010**, *46*, 6512. (b) Wei, P.; Atwood, D. A. *Inorg. Chem.* **1997**, *36*, 4060.

(18) (a) Tripathi, S. M.; Tandon, J. P. *Inorg. Nucl. Chem. Lett.* **1978**, *14*, 97. (b) Okada, M.; Hatori, O. PCT WO2011/013474 A1.

(19) Hadjaudis, E. *Mol. Eng.* **1995**, *5*, 301.

(20) The CSD 3D Graphics Search System v5.32 (November 2010): Allen, F. H. *Acta Crystallogr., Sect. B* **2002**, *58*, 380.

(21) Lewinski, J.; Zachara, J.; Stolarzewicz, P.; Dranka, M.; Kolodziejczyk, E.; Justyniak, I.; Lipkowski, J. *New J. Chem.* **2004**, *28*, 1320.

(11) (a) Wu, Q.; Esteghamatian, M.; Hu, N.-X.; Popovic, Z.; Enright, G.; Tao, Y.; D'Iorio, M.; Wang, S. *Chem. Mater.* **2000**, *12*, 79. (b) Qin, Y.; Kibur, I.; Shah, S.; Jäkle, F. *Org. Lett.* **2006**, *8*, 5227.

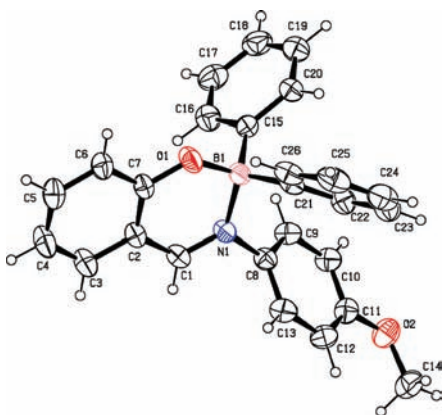


Figure 2. ORTEP view for **6** showing the atom-labeling scheme.

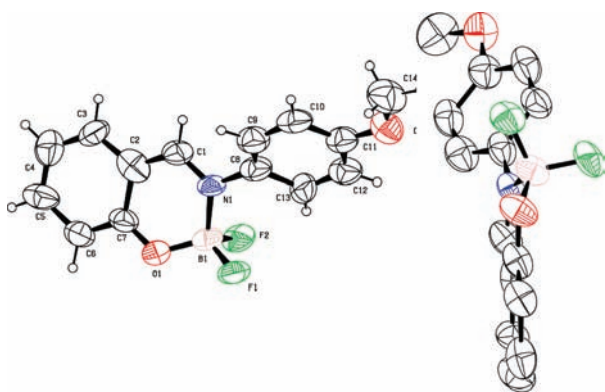
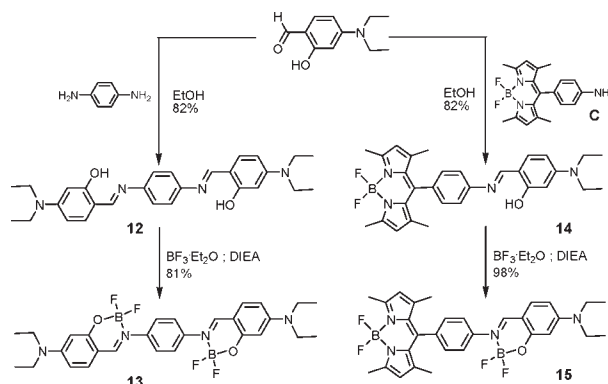


Figure 3. Left: ORTEP view for **5** showing the atom-labeling scheme. Right: perpendicular view to highlight the distortion at the B-atom.

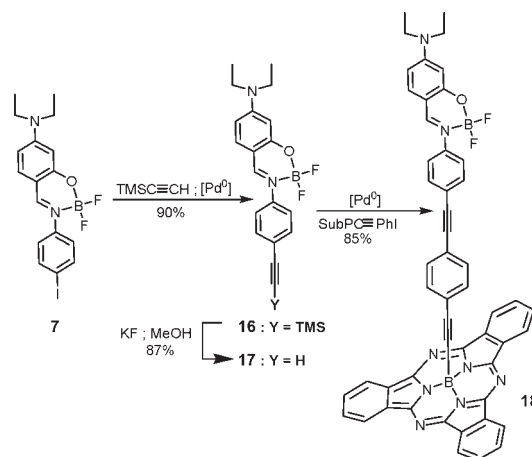
Developing upon these facile syntheses, we extended the method to dinuclear B-complexes (Scheme 2). The use of stoichiometric amounts of 4-diethylamino-2-hydroxy benzaldehyde provides derivatives **12** and **14** in 82% yield. Conversion to the respective B(III) complexes **13** and **15** proceeds efficiently, with no need for optimization.

In seeking to investigate a broader range of substituents, we found that a cross-coupling reaction using *Boranil* **7**, and promoted by low-valent palladium, is efficient using, for instance, trimethylsilylacetylene. No decomplexation of B in favor of Pd is observed, in keeping with the good stability of the B-complex. Compound **16** was found to be deprotected to the terminal alkyne using a slight excess of KF in polar solvents. The pivotal building block **17** was allowed to react with a prefunctionalized subphthalocyanine²² bearing a phenyliodo residue under

Scheme 2. Synthesis of Bis-*Boranils* and Borondipyromethane (BODIPY) Based *Boranil* Derivatives



Scheme 3. Synthesis of Functionalized Boranil Derivatives (SubPc accounts for *Boranil*)



standard conditions (Scheme 3). The stable and soluble dyad **18** was isolated in 85% yield. In **15** and **18**, the linkage of two photoactive moieties via an unsaturated spacer provides interesting spectroscopic features (*vide infra*).

The photophysical properties of the new dyes are summarized in Table 1. The absorption maxima and molar absorption coefficients (ϵ) were found to be dependent on the para substituents on both the phenol and imine sides and ranged from 372 to 443 nm and from 13 000 to 66 000 $\text{M}^{-1} \text{cm}^{-1}$, respectively. Note that the absorption spectra of dyes **5** and **6** present two transitions, reduced ϵ and low quantum yield compared to the other dyes (Table 1). This is typical of aggregation, further confirmed by a weak overlap between the excitation and absorption spectra (Figures S4,S5). On increasing the electronic density on the phenol side by adding a NEt_2 substituent in the para position (dyes **7**, **8**, and **10**), all the spectroscopic characteristics are dramatically improved. Switching from a fluoro to a phenyl group shifts the absorption by *ca.* 16 nm (compare **8/9** and **10/11**). By increasing the push-pull character along the main

(22) Camerel, F.; Ulrich, G.; Retailleau, P.; Ziessel, R. *Angew. Chem., Int. Ed.* **2008**, *47*, 8876.

(23) Olmsted, J. J. *Phys. Chem.* **1979**, *83*, 2581.

Table 1. Selected Optical Data Measured in Solution

dye	λ_{abs} (nm)	ϵ ($\text{M}^{-1}\cdot\text{cm}^{-1}$)	λ_{em} (nm)	Δ (cm^{-1})	ϕ_{f}^a	τ (ns)	solvent
5	342	12 600	471	8000	0.01	— ^b	Toluene
	372	13 000	471	5650	0.02	—	
6	338	9600	539	11 000	0.02	—	Toluene
	403	4200	539	8600	0.06	1.76	
7	403	69 000	455	2850	0.09	0.27	Toluene
8	396	44 000	445	2800	0.05	0.12	Toluene
9	409	32 000	492	4100	0.13	0.77	Toluene
10	427	66 000	474	2300	0.60	1.61	Toluene
10	422	49 000	473	2600	0.41	1.29	Et ₂ O
10	429	55 000	507	3600	0.13	0.78	THF
10	429	48 000	496	—	<0.01	—	MeCN
11	443	46 000	506	2800	0.61	2.73	Toluene
13	428	68 000	506	3600	0.90	1.14	Toluene
15	407	51 000	514	5100	0.45	—	Toluene
	504	75 000	514	—	0.49	2.81	
16	409	77 000	464	2900	0.09	0.29	Toluene
18	414	60 000	476	—	<0.01	—	Toluene
			574	6730	0.15	—	
	567	76 000	574	—	0.17	2.02	

^a Using quinine sulfate as reference $\Phi = 0.55$ in H_2SO_4 1N, $\lambda_{\text{ex}} = 366$ nm for dyes emitting below 480 nm; Rhodamine 6G as reference, $\Phi = 0.88$ in ethanol, $\lambda_{\text{ex}} = 488$ nm for dyes emitting between 480 and 570 nm; and cresyl violet as reference, $\Phi = 0.55$, $\lambda_{\text{ex}} = 546$ nm in ethanol for dyes emitting above 570 nm.^{23, b} Below detection limit.

molecular axis spanning over the ligand, a 55 nm bathochromic shift of the absorption is observed for **10** with respect to dye **5** (Figures 4a,S4). The absorption spectra consist of intraligand (IL) bands with additional $\pi-\pi^*$ transitions at 258 nm when using the BPh₂ fragment in Et₂O.

The simultaneous grafting of NEt₂ and NO₂ fragments onto the ligand provides bright luminescence with quantum yields reaching 61% for dyes **10** and **11** (Table 1). The high quantum yield does not depend on the nature of the B-substituents (compare **10** and **11** in toluene). The moderate Stokes shift from the longest-wavelength absorption to the most energetic emission is consistent with the assumption that the luminescence is fluorescence. This conclusion is supported by the observation that the emission is not quenched by oxygen and by the short lifetimes.

However, the shape of the emission band with several shoulders on the low energy side and the nonmirror symmetry with the absorption bands are suggestive of an intraligand charge transfer emissive state (ILCT).²⁴ By increasing the solvent polarity, the full width at half-maximum of the emission bands increases and the quantum yields dramatically decrease to insignificant values in polar acetonitrile (Table 1 and Figure S6). However, the dinuclear derivative **13** and the bipartite dyes **15** and **18** are less sensitive to the solvent polarity and less prone to a quantum yield decrease in polar solvents. This is a clear indication

(24) Kollmannsberger, M.; Rurack, K.; Resch-Genegr, U.; Daub, J. *J. Phys. Chem.* **1998**, *102*, 10211.

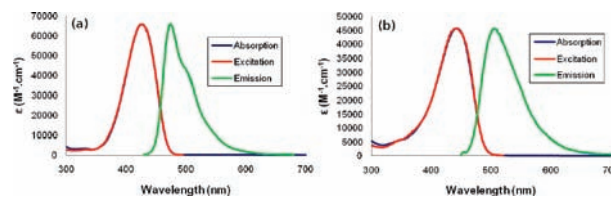


Figure 4. Absorption, emission, and excitation spectra of dyes (a) **10** and (b) **11** in toluene at rt.

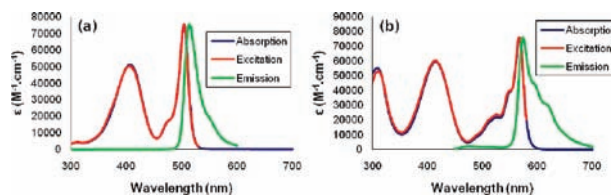


Figure 5. Absorption, emission, and excitation spectra of dyes **15** (a) and **18** (b) in toluene at rt.

that a much stronger ILCT character and larger dipole moment relative to the ground state are effective in leading to unusual complexes displaying optical properties dependent on the electronic modification of the chelate core.

These assumptions are further confirmed with the dinuclear dye **13** which exhibits a 90% quantum yield and the highest radiative rate of all dyes. In case of the dual dye **15**, the absorption profile is a linear combination of the absorption of the *Boranil* subunit and the Bodipy residues, a situation expected to arise due to the orthogonality of the phenyl ring. Interestingly, by irradiation in the N[^]O-boron fragment at 380 nm, quantitative energy transfer occurs, leading to the exclusive fluorescence of the Bodipy unit at 514 nm. This is supported by an excellent match between the excitation and absorption spectra over the entire wavelength range studied (Figure 5a).

Finally, similar results were obtained with the mixed dye **18**, where the absorption, emission, and excitation spectra confirm that the N[^]O-boron moiety could be used as an input energy antenna for cascade energy transfer to the fluorescent subphthalocyanine residue at 574 nm. Very little residual emission from the *Boranil* moiety is found at 476 nm probably due to a poorer spectral overlap of the *Boranil* subunit with the SubPc absorption (Figure 5b).

Efforts to increase the dipole moment in the excited state and thus to shift the optical properties in the red part of the spectrum are currently in progress.

Supporting Information Available. Synthetic procedures and analytical data. This material is available free of charge via the Internet at <http://pubs.acs.org>.